Chapter 3
Spin Relaxation in GaAs Based Quantum Dots for Security and Quantum Information Processing Applications

S. Prabhakar and R. Melnik

Abstract We report new three-dimensional modeling results of the band structure calculation of $GaAs/Al_{0.3}Ga_{0.7}As$ quantum dots (QDs) in presence of externally applied magnetic and electric fields along z-direction. We explore the influence of spin-orbit coupling in the effective g-factor of electrons in such QDs for possible application in security devices, encrypted data and quantum information processing. We estimate the relaxation rate in QDs caused by piezo-phonons.

3.1 Introduction

Several research proposals for the design of robust semiconductor spintronic devices for quantum logic gates in quantum information processing and security applications is based on the accurate manipulation of the effective g-factor of electrons with electric fields and estimation of the spin relaxation rate [14–16, 20]. One may expect a larger spin relaxation or decohenrence time than the gate operation time for the possible implementation of quantum dots devices in quantum information processing [1, 2]. Authors in Refs. [6, 11] have measured long spin relaxation times of 0.85 ms in GaAs QDs by pulsed relaxation rate measurements and 20 ms in InGaAs QDs by optical orientation measurements. These experimental studies in QDs confirm that the manipulation of spin-flip rates by spin-orbit coupling is important for the design of spintronics logic and other devices [7, 9, 16].

The spin-orbit coupling consists of the Rashba [3] and the linear Dresselhaus [5] terms that arise from structural inversion asymmetry along the growth direction and the bulk inversion asymmetry of the crystal lattice [1, 2, 24]. The electric and magnetic fields tunability of the electron g-factor in gated III-V semiconductor QDs with the Rashba and Dresselhaus spin-orbit couplings were explored in

S. Prabhakar (✉) • R. Melnik
MS2Discovery Interdisciplinary Research Institute, M ^{2}NeT Laboratory, Wilfrid Laurier University, Waterloo, ON, N2L 3C5 Canada
e-mail: sprabhakar@wlu.ca; rmelnik@wlu.ca

J. Bonča, S. Kruchinin (eds.), *Nanomaterials for Security*, NATO Science for Peace and Security Series A: Chemistry and Biology, DOI 10.1007/978-94-017-7593-9_3

Refs. [12, 15, 22–24]. It has also been noted that in-plane anisotropy due to gate potential also influences the effective Landé g-factor of electrons in QDs [15, 17, 27]. In this paper, we consider three-dimensional GaAs/$Al_{0.3}Ga_{0.7}$As conical QDs that are epitaxially formed at the heterojunction. We study the variation in the g-factor of electrons with electric and magnetic fields. We also estimate the phonon mediated spin-flip rate of electron spin states.

The paper is organized as follows. In Sect. 3.2, we provide a description of the theoretical model of three-Dimensional semiconductor QDs in presence of externally applied electric and magnetic fields. In Sect. 3.3, we give details of the diagonalization technique used for finding the eigenvalues and eigenstates for electrons in QDs. In Sect. 3.4, we discuss the dependency of the effective g-factor and spin relaxation rate with magnetic fields. Finally, in Sect. 3.5, we summarize our results.

3.2 Theoretical Model

We consider a GaAs/$Al_{0.3}Ga_{0.7}$As QD epitaxially formed at the heterojunction. In presence of magnetic field applied along z-direction, we write the total Hamiltonian of this quantum dot as: [1, 9, 19, 21, 24]

$$H = H_0 + H_{\mathrm{R}} + H_{\mathrm{D}}, \tag{3.1}$$

where H_{R} and H_{D} are Hamiltonians associated with the Rashba and Dresselhaus spin-orbit couplings and

$$H_0 = \frac{\mathbf{P}^2}{2m} + V(x, y, z) + eE_z z + \frac{1}{2} g_o \mu_{\mathrm{B}} \sigma_z B, \tag{3.2}$$

where $\mathbf{P} = \mathbf{p} + e\mathbf{A}$ is the kinetic momentum operator, $\mathbf{p} = -i\hbar(\partial_x, \partial_y, \partial_z)$ is the canonical momentum operator, $\mathbf{A} = B\,(-y, x, 0)$ is the vector potential, m is the effective mass of the electron in the conduction band, μ_{B} is the Bohr magneton and $\boldsymbol{\sigma} = (\sigma_x, \sigma_y, \sigma_z)$ are the Pauli spin matrices. Also, $V(x, y, z)$ is the confinement potential which is zero in the GaAs region and 0.3 eV in the barrier material, and E_z is the applied external field along z-direction. The Hamiltonians associated with the Rashba and Dresselhaus spin-orbit couplings can be written as [3, 5, 24]

$$H_{\mathrm{R}} = \frac{\alpha_{\mathrm{R}}}{\hbar} \left(\sigma_x P_y - \sigma_y P_x\right), \tag{3.3}$$

$$H_{\mathrm{D}} = \frac{\alpha_{\mathrm{D}}}{\hbar} \left(-\sigma_x P_x + \sigma_y P_y\right), \tag{3.4}$$

where the strengths of the Rashba and Dresselhaus spin-orbit couplings are characterized by the parameters α_{R} and α_{D}. They are given by

$$\alpha_{\mathrm{R}} = \gamma_{\mathrm{R}} eE, \quad \alpha_{\mathrm{D}} = 0.78\gamma_{\mathrm{D}} \left(\frac{2me}{\hbar^2}\right)^{2/3} E^{2/3}, \tag{3.5}$$

where γ_{R} and γ_{D} are the Rashba and Dresselhaus coefficients. Now we write $H|\Psi\rangle = \varepsilon|\Psi\rangle$ in terms of a coupled eigenvalue problem, consisting of two equations, in the basis states $|\psi_1\rangle$ and $|\psi_2\rangle$ as

$$\begin{aligned}
&\Big[-\frac{\hbar^2}{2m}\left(\partial_x^2 + \partial_y^2 + \partial_z^2\right) + \frac{1}{8}m\omega_c^2\left(x^2 + y^2\right) - \frac{i\hbar\omega_c}{2}\left(-y\partial_x + x\partial_y\right) + V(x,y,z) \\
&\quad + eE_z z + \frac{1}{2}g_0\mu_{\mathrm{B}}B\sigma_z\Big]|\psi_1\rangle + \Big[\alpha_{\mathrm{R}}eE_z\{\partial_x - i\partial_y + \frac{m\omega_c}{2\hbar}(x - iy)\}, \\
&\quad + \alpha_{\mathrm{D}}\Big\{ i\partial_x - \partial_y + \frac{m\omega_c}{2\hbar}(y - ix)\Big\}\Big]|\psi_2\rangle = \varepsilon|\psi_1\rangle,
\end{aligned} \tag{3.6}$$

$$\begin{aligned}
&\Big[-\frac{\hbar^2}{2m}\left(\partial_x^2 + \partial_y^2 + \partial_z^2\right) + \frac{1}{8}m\omega_c^2\left(x^2 + y^2\right) - \frac{i\hbar\omega_c}{2}\left(-y\partial_x + x\partial_y\right) + V(x,y,z) \\
&\quad + eE_z z + \frac{1}{2}g_0\mu_{\mathrm{B}}B\sigma_z\Big]|\psi_2\rangle + \Big[\alpha_{\mathrm{R}}eE_z\{-\partial_x + i\partial_y + \frac{m\omega_c}{2\hbar}(x + iy)\}, \\
&\quad + \alpha_{\mathrm{D}}\Big\{ -i\partial_x + \partial_y + \frac{m\omega_c}{2\hbar}(y + ix)\Big\}\Big]|\psi_1\rangle = \varepsilon|\psi_2\rangle,
\end{aligned} \tag{3.7}$$

where $\omega_c = eB/m$.

We now turn to the calculation of the phonon induced spin relaxation rate at absolute zero temperature. Following Ref. [18], the interaction between electrons and piezo-phonons can be written as [9, 10, 13, 29]

$$u_{ph}^{\mathbf{q}\alpha}(\mathbf{r},t) = \sqrt{\frac{\hbar}{2\rho V\omega_{\mathbf{q}\alpha}}}e^{i(\mathbf{q}\cdot\mathbf{r}-\omega_{q\alpha}t)}eA_{\mathbf{q}\alpha}b_{\mathbf{q}\alpha}^{\dagger} + \mathrm{H.c.} \tag{3.8}$$

Here, ρ is the crystal mass density, V is the volume of the QDs, $b_{\mathbf{q}\alpha}^{\dagger}$ creates an acoustic phonon with wave vector $\mathbf{q}$ and polarization $\hat{e}_\alpha$, where $\alpha = l, t_1, t_2$ are chosen as one longitudinal and two transverse modes of the induced phonon in the dots. Also, $A_{\mathbf{q}\alpha} = \hat{q}_i\hat{q}_k e\beta_{ijk}e_{\mathbf{q}\alpha}^{j}$ is the amplitude of the electric field created by phonon strain, where $\hat{\mathbf{q}} = \mathbf{q}/q$ and $e\beta_{ijk} = eh_{14}$ for $i \neq k, i \neq j, j \neq k$. The polarization directions of the induced phonon are $\hat{e}_l = (\sin\theta\cos\phi, \sin\theta\sin\phi, \cos\theta)$,

$\hat{e}_{t_1} = (\cos\theta\cos\phi, \cos\theta\sin\phi, -\sin\theta)$ and $\hat{e}_{t_2} = (-\sin\phi, \cos\phi, 0)$. Based on the Fermi Golden Rule, the phonon induced spin transition rate in the QDs is given by [10, 24]

$$\frac{1}{T_1} = \frac{2\pi}{\hbar}\int \frac{d^3\mathbf{q}}{(2\pi)^3}\sum_{\alpha=l,t}|M(\mathbf{q}\alpha)|^2\delta\left(\hbar s_\alpha \mathbf{q} - \varepsilon_f + \varepsilon_i\right), \tag{3.9}$$

where s_l,s_t are the longitudinal and transverse acoustic phonon velocities in QDs. Under the dipole approximation, we write (3.9) as [10, 25]

$$\frac{1}{T_1} = c\left(|M_x|^2 + |M_y|^2 + |M_z|^2\right), \tag{3.10}$$

where

$$c = \frac{2(eh_{14})^2\left(\varepsilon_f - \varepsilon_i\right)^3}{35\pi\hbar^4\rho}\left(\frac{1}{s_l^5} + \frac{4}{3}\frac{1}{s_t^5}\right), \tag{3.11}$$

$$M_x = \langle\psi_i|x|\psi_f\rangle, \tag{3.12}$$

$$M_y = \langle\psi_i|y|\psi_f\rangle, \tag{3.13}$$

$$M_z = \langle\psi_i|z|\psi_f\rangle. \tag{3.14}$$

In the above expression, we use $c = c_l I_{xl} + 2c_t I_{xt}$, where $c_\alpha = \frac{q^2e^2}{(2\pi)^2\hbar^2 s_\alpha}|\varepsilon_{q\alpha}|^2$, $|\varepsilon_{q\alpha}|^2 = \frac{q^2\hbar}{2\rho\omega_{q\alpha}}$. For longitudinal phonon modes similar to Refs. [7, 10], we have $|A_{q,l}|^2 = 36h_{14}^2\cos^2\theta\sin^4\theta\sin^2\phi\cos^2\phi$. Likewise, for transverse phonon modes, we have $|A_{q,t}|^2 = 2h_{14}^2[\cos^2\theta\sin^2\theta + \sin^4\theta\left(1 - 9\cos^2\theta\right)\sin^2\phi\cos^2\phi]$.

3.3 Computational Method

The geometry of GaAs conical QDs with wetting layer is shown in Fig. 3.1. The QDs are surrounded by host barrier material $Al_{0.3}Ga_{0.7}As$. We diagonalize the total Hamiltonian H using the finite-element method [4]. In typical examples reported here, the geometry contains on the order of 56729 elements. We impose Dirichlet boundary conditions at the outside boundaries to let the wavefunction to vanish and Neumann boundary conditions at the internal boundaries to let the wavefunction to follow continuity equation. Then we find eigenvalues and eigenfunctions by solving two coupled equations (3.6) and (3.7).

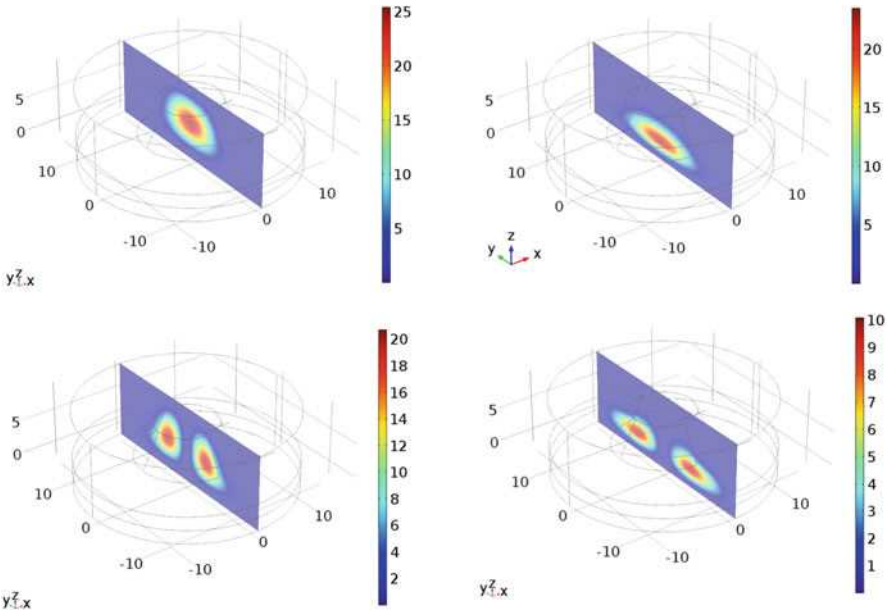

Fig. 3.1 Illustration of ground state wavefunctions (*upper panel*) and first excited state wavefunctions (*lower panel*) of electrons in GaAs/AlGaAs QDs. *Left column* QD wavefunctions correspond to the externally applied electric field, $E_z = 0.001$ V/nm, while *right column* QD wavefunctions correspond to the externally applied electric field, $E_z = 0.1$ V/nm. Evidently, penetration of wavefunctions from the QD region to the barrier materials leads to the variation in the Lande g-factor of electrons that can be utilized to design spintronic devices for security and quantum information processing

3.4 Results and Discussions

In Fig. 3.1, we have plotted probability distribution, $|\psi_1|^2 + |\psi_2|^2$ (arbitrary unit) of ground (upper panel) and first excited state (lower panel) wavefunctions of electron at $E_z = 0.001$ V/nm (left panel) and $E_z = 0.1$ V/nm (right panel). As we can see, the penetration of electron wavefunctions into the barrier material is enhanced for larger values of the applied electric field along z-direction. This leads to the variation in the effective g-factor (see also Fig. 3.3) of electrons in GaAs/$Al_{0.3}Ga_{0.7}As$ QDs that can be utilized to design quantum logic gates for applications in security and quantum information processing. In Fig. 3.2, we have plotted a cross section along z-direction of the edge potential and probability distribution ($|\psi_1|^2 + |\psi_2|^2$) of ground state

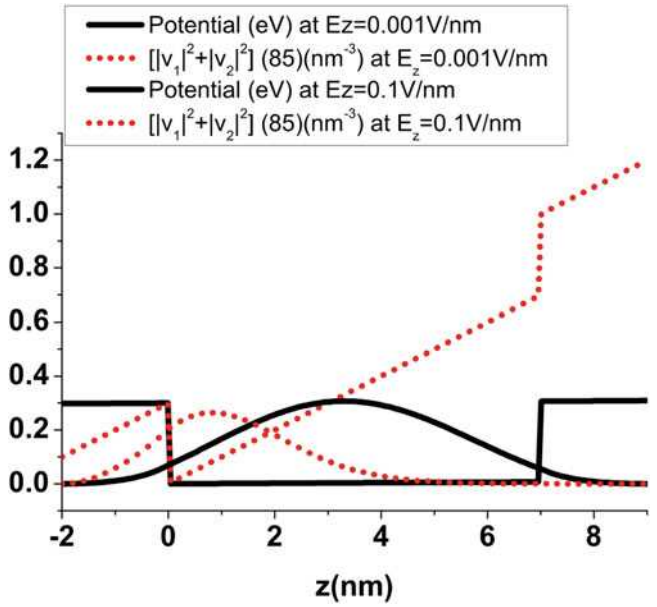

Fig. 3.2 Conduction band edge and its corresponding normalized wavefunctions vs distance from $GaAs/Al_{0.3}Ga_{0.7}As$. Again, penetration of wavefunctions in the barrier material at large electric fields can be seen (also see Ref. [8])

wavefunctions of electrons at $E_z = 0.001\,\mathrm{V/nm}$ (left panel) and $E_z = 0.1\,\mathrm{V/nm}$ (right panel). Here we again see that the penetration of electron wavefunctions into the barrier material is enhanced for larger values of the applied electric field along z-direction (for experiment results, see Ref. [8]). In Fig. 3.3 (upper panel), we have plotted the effective g-factor, $g = (\varepsilon_1 - \varepsilon_2)/\mu_B B$ of electron vs magnetic fields. Here, the variation of effective g-factor of electrons in quantum dots with electric field can be seen and can be applied to make quantum logic gates for application in spintronic devices. At large magnetic fields, we find the level crossing due to admixture of spin and orbital states (see lower panel of Fig. 3.3). In Fig. 3.4, we have plotted piezo-phonon mediated spin and orbital relaxation vs magnetic fields in $GaAs/Al_{0.3}Ga_{0.7}As$ QDs at $E_z = 0.1\,\mathrm{V/nm}$. We see that the relaxation rate is enhanced with magnetic fields and can approach to the orbital relaxation rate at large magnetic fields where the decoherence time is greatly reduced due to the level crossing of orbital and spin states. Such an ideal location should be avoided during the design of spintronic devices for application in security and quantum information processing (Table 3.1).

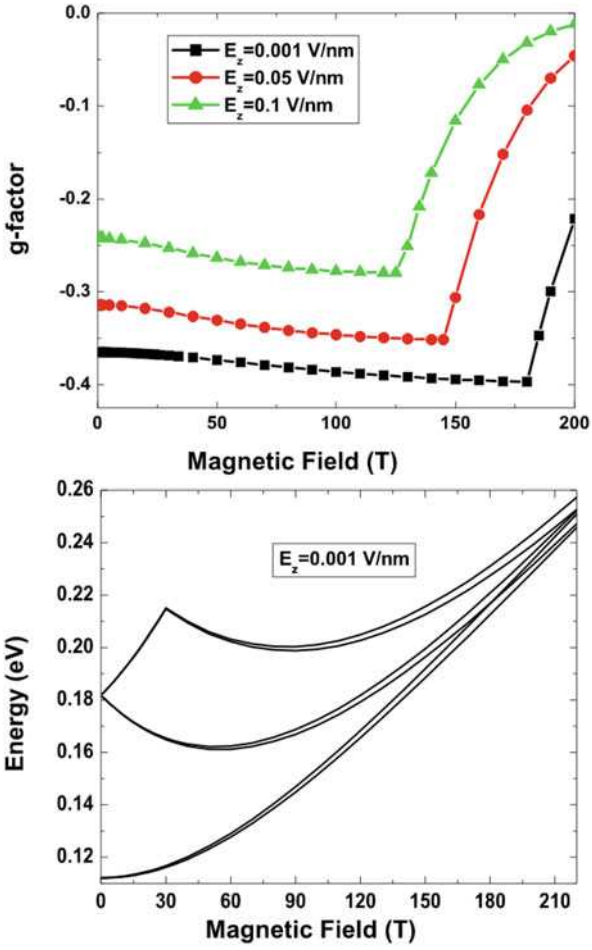

Fig. 3.3 (*upper*) Electron effective g-factor vs magnetic field in $GaAs/Al_{0.3}Ga_{0.7}As$ QDs. Level crossing can be observed at large magnetic fields which vary with the applied external electric fields along z-direction. (*lower*) Band diagram of electron in $GaAs/Al_{0.3}Ga_{0.7}As$ QDs vs magnetic field. The band crossing is seen at large magnetic field, $B \approx 185\,\mathrm{T}$

3.5 Conclusion

Based on finite element implementation, we have provided three-dimensional modeling results for the tuning of the effective g-factor of electrons with spin orbit coupling in $GaAs/Al_{0.3}Ga_{0.7}As$ QDs and shown that the level crossing can be observed at large magnetic fields due to the admixture of spin and orbit states. We also estimated the relaxation rate caused by piezo-phonon and shown that the spin-hot spot can be observed at the level crossing point. Decoherence time is greatly reduced at the level crossing point. Thus, We suggest to avoid such an ideal location in the design of GaAs based QD devices for possible applications in spintronics, security, encrypted data and quantum information processing.

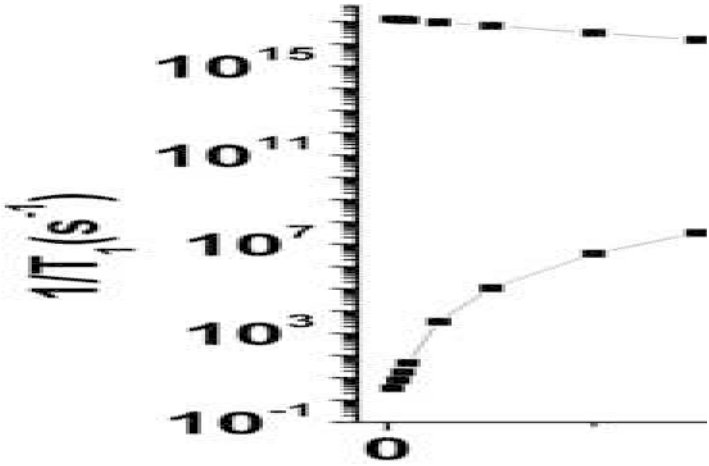

Fig. 3.4 Piezo-phonon mediated spin relaxation vs magnetic fields in GaAs/$Al_{0.3}Ga_{0.7}As$ QDs at $E_z = 0.1\,V/nm$

Table 3.1 The material constants used in our calculations are taken from Refs. [19, 26, 28]

Parameters	GaAs	$Al_{0.3}Ga_{0.7}As$
g_0	−0.44	0.4
m	$0.067m_0$	$0.088m_0$
α_R [nm^2]	0.044	0.022
α_D [eVnm^3]	0.026	0.0076
eh_{14} [10^{-5} erg/cm]	2.34	0.54
s_l [10^5 cm/s]	5.14	
s_t [10^5 cm/s]	3.03	
ρ [g/cm^3]	5.3176	

References

1. Bulaev DV, Loss D (2005) Spin relaxation and decoherence of holes in quantum dots. Phys Rev Lett 95:076805
2. Bulaev DV, Loss D (2005) Spin relaxation and anticrossing in quantum dots: Rashba versus dresselhaus spin-orbit coupling. Phys Rev B 71:205324
3. Bychkov YA, Rashba EI (1984) Oscillatory effects and the magnetic susceptibility of carriers in inversion layers. J Phys C: Solid State Phys 17:6039
4. Comsol Multiphysics version 5.1. www.comsol.com
5. Dresselhaus G (1955) Spin-orbit coupling effects in zinc blende structures. Phys Rev 100:580
6. Elzerman JM, Hanson R, Willems van Beveren LH, Witkamp B, Vandersypen LMK, Kouwenhoven LP (2004) Single-shot read-out of an individual electron spin in a quantum dot. Nature 430:431
7. Golovach VN, Khaetskii A, Loss D (2004) Phonon-induced decay of the electron spin in quantum dots. Phys Rev Lett 93:016601

8. Jiang HW, Yablonovitch E (2001) Gate-controlled electron spin resonance in GaAs/$Al_xGa_{1-x}As$ heterostructures. Phys Rev B 64:041307
9. Khaetskii AV, Nazarov YV (2000) Spin relaxation in semiconductor quantum dots. Phys Rev B 61:12639
10. Khaetskii AV, Nazarov YV (2001) Spin-flip transitions between zeeman sublevels in semiconductor quantum dots. Phys Rev B 64:125316
11. Kroutvar M, Ducommun Y, Heiss D, Bichler M, Schuh D, Abstreiter G, Finley, JJ (2004) Optically programmable electron spin memory using semiconductor quantum dots. Nature 432:81
12. Nowak MP, Szafran B, Peeters FM, Partoens B, Pasek WJ (2011) Tuning of the spin-orbit interaction in a quantum dot by an in-plane magnetic field. Phys Rev B 83:245324
13. Olendski O, Shahbazyan TV (2007) Theory of anisotropic spin relaxation in quantum dots. Phys Rev B 75:041306
14. Prabhakar S, Melnik R (2015) Electric field control of spin splitting in III–V semiconductor quantum dots without magnetic field. Eur Phys J B 88:273
15. Prabhakar S, Raynolds JE (2009) Gate control of a quantum dot single-electron spin in realistic confining potentials: anisotropy effects. Phys Rev B 79:195307
16. Prabhakar S, Raynolds J, Inomata A, Melnik R (2010) Manipulation of single electron spin in a gaas quantum dot through the application of geometric phases: the Feynman disentangling technique. Phys Rev B 82:195306
17. Prabhakar S, Raynolds JE, Melnik R (2011) Manipulation of the landé *g* factor in inas quantum dots through the application of anisotropic gate potentials: exact diagonalization, numerical, and perturbation methods. Phys Rev B 84:155208
18. Prabhakar S, Melnik R, Bonilla LL (2012) The influence of anisotropic gate potentials on the phonon induced spin-flip rate in GaAs quantum dots. Appl Phys Lett 100:023108
19. Prabhakar S, Melnik R, Bonilla LL (2013) Electrical control of phonon-mediated spin relaxation rate in semiconductor quantum dots: Rashba versus dresselhaus spin-orbit coupling. Phys Rev B 87:235202
20. Prabhakar S, Melnik R, Bonilla L (2014) Gate control of Berry phase in III–V semiconductor quantum dots. Phys Rev B 89:245310
21. Prabhakar S, Melnik R, Inomata A (2014) Geometric spin manipulation in semiconductor quantum dots. Appl Phys Lett 104:142411
22. Pryor CE, Flatté ME (2006) Landé *g* factors and orbital momentum quenching in semiconductor quantum dots. Phys Rev Lett 96:026804
23. Pryor CE, Flatté ME (2007) Erratum: Landé *g* factors and orbital momentum quenching in semiconductor quantum dots. Phys Rev Lett 99:179901
24. Sousa R, Sarma S (2003) Gate control of spin dynamics in III-V semiconductor quantum dots. Phys Rev B 68:155330
25. Stano P, Fabian J (2006) Orbital and spin relaxation in single and coupled quantum dots. Phys Rev B 74:045320
26. Stern F, Sarma S (1984) Electron energy levels in GaAs-$Ga_{1-x}Al_xAs$ heterojunctions. Phys Rev B 30:840
27. Takahashi S, Deacon RS, Yoshida K, Oiwa A, Shibata K, Hirakawa K, Tokura Y, Tarucha S (2010) Large anisotropy of the spin-orbit interaction in a single InAs self-assembled quantum dot. Phys Rev Lett 104:246801
28. von Allmen P (1992) Conduction subbands in a GaAs/$Al_xGa_{1-x}As$ quantum well: comparing different k·p models. Phys Rev B 46:15382
29. Woods LM, Reinecke TL, Lyanda-Geller Y (2002) Spin relaxation in quantum dots. Phys Rev B 66:161318

NATO Science for Peace and Security Series - A:
Chemistry and Biology

Nanomaterials for Security

Edited by
Janez Bonča
Sergei Kruchinin

Springer

NATO OTAN

This publication is supported by:

The NATO Science for Peace and Security Programme

NATO Science for Peace and Security Series

This Series presents the results of scientific meetings supported under the NATO Programme: Science for Peace and Security (SPS).

The NATO SPS Programme supports meetings in the following Key Priority areas: (1) Defence Against Terrorism; (2) Countering other Threats to Security and (3) NATO, Partner and Mediterranean Dialogue Country Priorities. The types of meetings supported are generally "Advanced Study Institutes" and "Advanced Research Workshops". The NATO SPS Series collects together the results of these meetings. The meetings are co-organized by scientists from NATO countries and scientists from NATO's "Partner" or "Mediterranean Dialogue" countries. The observations and recommendations made at the meetings, as well as the contents of the volumes in the Series, reflect those of participants and contributors only; they should not necessarily be regarded as reflecting NATO views or policy.

Advanced Study Institutes (ASI) are high-level tutorial courses to convey the latest developments in a subject to an advanced-level audience.

Advanced Research Workshops (ARW) are expert meetings where an intense but informal exchange of views at the frontiers of a subject aims at identifying directions for future action.

Following a transformation of the programme in 2006, the Series has been re-named and re-organised. Recent volumes on topics not related to security, which result from meetings supported under the programme earlier, may be found in the NATO Science Series.

The Series is published by IOS Press, Amsterdam, and Springer, Dordrecht, in conjunction with the NATO Emerging Security Challenges Division.

Sub-Series

A.	Chemistry and Biology	Springer
B.	Physics and Biophysics	Springer
C.	Environmental Security	Springer
D.	Information and Communication Security	IOS Press
E.	Human and Societal Dynamics	IOS Press

http://www.nato.int/science
http://www.springer.com
http://www.iospress.nl

Series A: Chemistry and Biology

Nanomaterials for Security

edited by

Janez Bonča
J. Stefan Institute, Ljubljana, Slovenia

and

Sergei Kruchinin
Bogolyubov Institute for Theoretical Physics, Kiev, Ukraine

Published in Cooperation with NATO Emerging Security Challenges Division

Proceedings of the NATO Advanced Research Workshop on
Nanomaterials for Security
Odessa, Ukraine
August 30–September 3, 2015

Library of Congress Control Number: 2016946179

ISBN 978-94-017-7594-6 (PB)
ISBN 978-94-017-7591-5 (HB)
ISBN 978-94-017-7593-9 (e-book)
DOI 10.1007/978-94-017-7593-9

Published by Springer,
P.O. Box 17, 3300 AA Dordrecht, The Netherlands.

www.springer.com

Printed on acid-free paper

Contents

Part I Nanomaterials

1 Atomic Collapse in Graphene 3
D. Moldovan and F.M. Peeters

2 Fluorination Clusters on Graphene Resolved by Conductive AFM 19
A. Mishchenko, A. Eckmann, I.V. Grigorieva, and K.S. Novoselov

3 Spin Relaxation in GaAs Based Quantum Dots for Security and Quantum Information Processing Applications 25
S. Prabhakar and R. Melnik

4 Very Sensitive Nanocalorimetry of Small Mass Systems and Glassy Materials 35
J.-L. Garden, A. Tavakoli, T. Nguyen-Duc, A. Frydman, M. Laarraj, J. Richard, and O. Bourgeois

5 Phase Conversion of Y-Ba-Cu-O Thin Films by Super-Oxygenation and Cu-Enrichment 45
H. Zhang, N. Gauquelin, C. Mcmahon, D.G. Hawthorn, G.A. Botton, and J.Y.T. Wei

6 Strong-Coupling Diagram Technique for Strong Electron Correlations 57
A. Sherman

7 Spin-Dependent Transport of Carbon Nanotubes with Chromium Atoms 67
S.P. Kruchinin, S.P. Repetsky, and I.G. Vyshyvana